EVOLUTION & DEVELOPMENT 14:4, 326–337 (2012)
DOI: 10.1111/j.1525-142X.2012.00551.x

Developmental dissociation in morphological evolution of the stickleback opercle

Charles B. Kimmel,[a,*] Paul A. Hohenlohe,[b,1] Bonnie Ullmann,[a] Mark Currey,[b] and William A. Cresko[b]

[a] Institute of Neuroscience, University of Oregon, Eugene, OR, 97403, USA
[b] Institute of Ecology and Evolution, University of Oregon, Eugene, OR, 97403, USA

*Author for correspondence (email: kimmel@uoneuro.uoregon.edu)
[1]Present address: Department of Biological Sciences and Institute of Bioinformatics and Evolutionary Studies, University of Idaho, Moscow, ID, 83844, USA

SUMMARY Oceanic threespine sticklebacks have repeatedly and independently evolved new morphologies upon invasions of freshwater habitats. A consistent derived feature of the freshwater form across populations and geography is a shape change of the opercle, a large early developing facial bone. We show that the principal multivariate axis describing opercle shape development from the young larva to the full adult stage of oceanic fish matches the principal axis of evolutionary change associated with relocation from the oceanic to freshwater habitat. The opercle phenotype of freshwater adults closely resembles the phenotype of the bone in juveniles. Thus, evolution to the freshwater condition is in large part by truncation of development; the freshwater fish do not achieve the full ancestral adult bone shape. Additionally, the derived state includes dissociated ontogenetic changes. Dissociability may reflect an underlying modular pattern of opercle development, and facilitate flexibility of morphological evolution.

INTRODUCTION

What are key features in the ways that development works that might facilitate or, conversely, restrict evolutionary change? One of these is the principle of dissociability, the doctrine that seemingly integrated developmental processes can be separated from one another (Needham 1933). Dissociability has often been discussed in the context of heterochrony, in particular the separation of size and shape by changes in developmental timing (Gould 1977). However, dissociation might just as well apply to aspects of shape development. For example, consider the mammalian jaw—made from just a single bone, the dentary, which varies widely in shape among different mammalian groups. Such shape differences likely have their basis in dissociation of features of development (including growth) among different regions of this single bone. The mandible is thought to arise from several discrete mesenchymal condensations (Atchley and Hall 1991), and is composed of at least two modules (developmental, or perhaps functional), units that are strongly integrated internally, but are fairly autonomous from other modules (Cheverud 1996; Zelditch et al. 2008; Klingenberg 2009). Regional semiautonomy provided by modular development might facilitate evolutionary dissociability (Raff 1996; Wagner 1996; Raff and Raff 2000).

We also focus on a single skull bone, the opercle, supporting the gill cover in teleosts (Gregory 1933) as another potentially useful system for learning about connections between developmental dissociability and evolutionary change. The opercle of the zebrafish provides a model for morphogenesis and molecular regulation. Under control of a number of regulatory genes (Kimmel et al. 2003; Miller et al. 2007b; Talbot et al. 2010), the opercle arises from a single mesenchymal condensation, and then dynamically forms a triangular larval bone (Kimmel et al. 2010). In a stage-specific manner, each of the three triangle edges grow and reshape by local recruitments of osteoblasts, a pattern that suggested an underlying modularity (Kimmel et al. 2010). Notably, the Indian hedgehog (Ihha) protein normally functions as a local signal from osteoblasts to preosteoblasts along one of these edges, and in *ihha* mutants the ventral opercle edge (but not the other edges) develops abnormally (Huycke et al. 2012). Such dissociation of development, between the *ihha*-dependent edge and the other parts of the bone, and revealed by molecular genetic analysis, supports the hypothesis of modularity. The Indian hedgehog signal would provide for the initiation of development, and possibly the maintenance of a single module.

The opercle of the threespine stickleback provides a model for evolution at the level of this single bone organ. During at least the past 10 million years, and across the northern hemisphere, oceanic sticklebacks have repeatedly evolved into resident freshwater forms (Bell and Foster 1994), and changes in opercle shape have accompanied many morphological

divergences that distinguish the two life history forms (Kimmel et al. 2005, 2008). The opercles of extant oceanic fish are very uniform in shape irrespective of local population (Kimmel et al. 2012) and provide a robust surrogate for the ancestral morphotype (Bell and Foster 1994; Raeymaeker et al. 2005, 2007; Makinen et al. 2006; Hohenlohe et al. 2010). Opercle morphologies among different freshwater stickleback are more divergent, yet show a prominent signal of parallel shape evolution from the oceanic form in geographical locations as remote from one another as Alaska and Iceland (Kimmel et al. 2012). Furthermore, the evolutionary change between oceanic and freshwater opercle morphology can occur extremely rapidly, within just tens of years (Arif et al. 2009; Kimmel et al. 2012).

Here, we examine the developmental basis of opercle evolutionary change in form. Our starting point is to explore an observation that evolutionary divergence is accompanied by a change in developmental allometry (Kimmel et al. 2008). Specifically, we observed dissociation between bone shape and size, in comparisons of juvenile and adult sticklebacks from Alaskan oceanic and lake populations. Were this same allometric change to occur generally in independently evolved populations of freshwater fish, then we should find that evolutionary allometry across freshwater populations matches developmental allometry in the Alaskan freshwater fish. We examine this prediction here, and show that it is confirmed. This result motivated a more thorough analysis of ontogeny than was performed previously. Sampling a 2-year period of opercle development—from early larval stage through adult stage—we show that in the derived state, the major axis of shape development becomes pedomorphically shortened. However, the new developmental trajectory does not result from a single, uniform timing change. Rather, in accord with recent, more nuanced views of the role of heterochrony in evolution, we see dissociations among regions of the bone. This dissociability likely has a modular basis, and might have facilitated divergent evolution including freshwater habitats with special ecologies.

MATERIALS AND METHODS

Datasets

To study allometry across populations of wild-captured fish, we performed additional analyses on the same dataset used recently for opercle shape characterization (Kimmel et al. 2012), here including opercle size. The previous paper describes the collections; briefly, the set includes 744 Alizarin Red stained adult fish from 22 populations each including about 30 individuals. The populations include samples from the oceanic freshwater habitats in Iceland and from four regions of Western Coastal North America—including in particular South Central Alaska.

To compare opercle shape and size development, we grew fish from lab strains originating from two localities in South-Central Alaska, Rabbit Slough (oceanic habitat) and Boot Lake (freshwater habitat). Our study was cross-sectional, utilizing separate sets of 20–30 fish for each of five developmental stages for both habitats (total: 285 individuals). Each set originated from a single pair mating, and was raised in separate aquaria, with a salinity of 1 ppt, mimicking a slightly brackish freshwater environment. Full details of husbandry are available (http://stickleback.uoregon.edu/index.php/). The sets for the adult-stage opercles representing both habitats and the set for the juvenile-stage Rabbit Slough fish were the same as studied previously (Kimmel et al. 2008, 2012). All work conformed to University of Oregon IACUC requirements.

At the two youngest developmental stages, 10 and 14 days postfertilization (dpf), the opercles are only very lightly mineralized, and we used highly sensitive live confocal imaging (Zeiss LSM5 Pascal confocal microscope, New York, NY, USA) of fish vitally stained for 1 or 2 h with 50 μg/ml of Alizarin Red S to reveal the full extent of mineralization (Kimmel et al., 2005, 2010). The fish were mounted to obtain a left-side view of the flat "face" of the opercle, a confocal z-series stack of images taken (Kimmel et al. 2010), and the bone shape analyzed in a single projection made from the stack. For all of the other stages, single images were taken of the left side of the head of formaldehyde-preserved and Alizarin Red stained fish with a Nikon E4500 digital camera (Melville, NY, USA) mounted on a Nikon SMZ1500 stereomicroscope (Kimmel et al. 2005, 2008).

Morphometric analyses

Landmarks along the edges of the opercles (Fig. 1) were digitized from micrographs as described (Rohlf 2008a; Kimmel et al. 2008). The configurations from both the adult and developmental datasets ($n = 1029$) were all Procrustes superimposed and aligned together in tpsRelw (Rohlf 2008b), the single alignment allowing direct comparisons between the two datasets (see below). As in the previous work, four of the nine landmarks (numbers 4, 5, 6, 8; see Fig. 1) were treated as sliding semilandmarks. Each sliding landmark was placed half way along a measured interval of the bone contour between the adjacent two landmarks, and the sliding of these landmarks was performed in tpsRelw. Ten nonzero Principal Components (PCs) were computed from the Procrustes residuals of the aligned landmarks in JMP (SAS Institute Inc., v. 8, Cary, NC, USA) in two separate Principal Component Analyses (PCAs): The first, yielding $PC1_a$-10_a (the "a" denoting adult) is computed from the wild-captured adults ($n = 744$) exactly as in the previous study utilizing the same samples (Kimmel et al. 2012). The second, $PC1_d$-10_d (the "d" denoting development) is computed from the collected set of

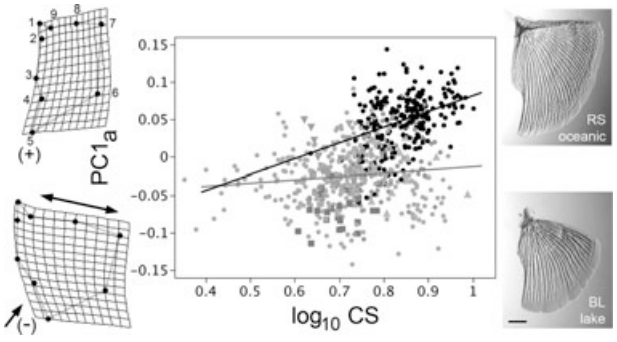

Fig. 1. Evolutionary (phyletic) opercle allometry differs in sticklebacks that have diverged from oceanic to freshwater habitats. The data points on the allometric (shape vs. size) plot show the first principal component of opercle shape ($PC1_a$, explaining 46% of the total variation in shape) regressed on opercle size (centroid size, CS) of individual adult fish ($n = 744$) collected in the wild from 22 separate populations, with black points representing fish from 8 oceanic populations, and the gray symbols representing fish from 14 freshwater populations; we recently described in detail the opercle shapes (but not sizes) from the same dataset (Kimmel et al., 2012). Distinctive symbols are used for three freshwater populations singled out below, Boot Lake (Alaska, squares), Skorraddalsvatn Lake (Iceland, downward pointing triangles), and Paxton Lake (benthic population, from British Columbia, upward pointing triangles). Ordinary least squares (OLSs) regression lines are shown, black for the oceanic fish and gray for the freshwater fish, the slopes differ significantly (see text). The thin plate spline diagrams to the left show shape deformations at positive (upper, corresponding to the oceanic morph) and negative (lower, corresponding to the freshwater morph) extremes along the $PC1_a$ axis. Double-headed and single-headed arrows show the characteristic dilation-diminution deformation in opercle shape at low $PC1_a$, and associated with evolution to freshwater habitats. The micrographs to the right show examples of Alizarin Red stained opercles dissected from Rabbit Slough (RS, oceanic) and Boot Lake (BL, freshwater) fish. Scale bar: 1 mm.

five developmental stages of lab-reared fish originating from Rabbit Slough ($n = 124$). PC scores were assigned secondarily, to fish not included in these computations (e.g., both PC_a and PC_d scores were so projected to the developmental set of fish from Boot Lake, even though these fish were excluded in the computation of the scores). This approach allows any and all of the samples to be examined together in the same trait-spaces delineated either by variation across the evolutionary or the ancestral developmental landscapes. Graphic visualizations of the deformations of the landmark configurations were obtained from tpsRelW and tpsSpline (Rohlf 2004).

Multivariate regressions using the Procrustes aligned residuals from the developmental datasets (Rabbit Slough and Boot), centroid sizes (CSs), and time (days postfertilization) were carried out in MorphoJ (v. 1.02f, Klingenberg 2011). Ordinary least square (OLS) bivariate regression analyses were carried out in JMP, and reduced major axis (RMA) regression analyses were done with the SMATR package in R (Warton et al. 2006).

Modularity evaluation

We examined the hypothesis that the opercle consists of dorsal and ventral modules, using a method based on partial least squares analysis, described by Klingenberg (2009) and implemented in MorphoJ. We made new landmark configurations of eight landmarks (four dorsal and four ventral), none of which were sliding landmarks, and positioned as shown in the Results section below. Although these eight landmark configurations do not show the opercle shapes as adequately as the nine landmark configurations used for the other analyses, avoidance of sliding landmarks is required for this test because sliding landmarks introduce artificial covariances (e.g., see Zelditch et al. 2004). We combined the datasets for the juvenile-stage opercles from both Boot Lake (BL) and Rabbit Slough (RS) ($n = 30$ individuals each), and, from the Procrustes transformed coordinates we generated a covariance matrix using the "pooled within group" option featured in MorphoJ. Using this option, let us examine the covariance structure, and potential modularity structure, which is shared by both populations, rather than the differences between the two populations. For permutation analysis, the evaluation of all possible contiguous partitions of the configuration into two blocks of equal size to the hypothetical module, we assigned adjacencies that better accounted for the opercle anatomy than the default adjacency profile provided by MorphoJ, DeLaunay triangulation, following recommendations provided by Klingenberg (2009). We removed connections outside of the contours of the bone, and filled in additional quadrilaterals of nearby landmarks within the bone contours. The adjacency profile used is also shown in the Results section.

RESULTS

Evolutionary dissociation between opercle shape and size

In sticklebacks that have independently colonized freshwater habitats, opercle shapes evolve in parallel (Kimmel et al. 2012). This habitat-associated divergence is along the major axis through a multivariate phenotypic space we described by PCA. The axis, $PC1_a$, captures 46% of the total shape variation in a dataset that includes 8 geographically widespread oceanic and 14 freshwater populations. The change in the negative direction along PC1 includes a diminution of the ventral (lower) region of the bone (single-headed arrow, Fig. 1), covarying with a dilation of the dorsal (upper) region (double headed arrow). The second axis, $PC2_a$, describes

divergences among particular freshwater populations (Kimmel et al. 2012) that we discuss further below.

We had not described opercle size–shape relationships for these populations (Kimmel et al. 2012). Here, we show that regressions of $PC1_a$ on opercle size, represented by log CS, yield different slopes for the two habitats (Fig. 1). The relationships are noisy (e.g., $R^2 = 0.15$ for the oceanic OLS regression), as might be expected in part because 22 different populations contribute to this plot. Nevertheless, the oceanic fish show significant evolutionary allometry (slope = 0.210 $\pm$ 0.032 [SE], OLS), whereas the relationship for the freshwater is isometric, or nearly so (slope = 0.043 $\pm$ 0.017). Furthermore, the two slopes differ significantly from one another (OLS slopes examined by ANCOVA; $F_{1740} = 17.6$; $P < 0.0001$, and RMA slopes examined by permutation; $P < 0.0001$).

Comparing this result and our previous findings of a similar change in size–shape relationships during maturation of juvenile sticklebacks of Alaskan origin (Kimmel et al. 2008), we hypothesized that allometric changes along the course of development underlie shape divergence of the opercle in these widespread populations, as we further examine.

Evolution includes a prominent truncation of shape development

We carried out a cross-sectional study using laboratory-reared fish derived from wild-captured oceanic (Rabbit Slough, RS) and freshwater (Boot Lake, BL) populations from SE Alaska to explore a potential developmental correlate of the allometric relationships just described. Procrustes distances, univariate measures of the shape RS–BL disparities, are significantly different at each time point along of the series of five developmental stages, sampled during a period of 2 years (Table 1, first row, "stage-matched"). The developmental changes are evidently complex, not following von Baer's rule (1836), according to which the earliest stage should show the most RS–BL similarity. Rather, the 30 dpf, opercle shapes are most similar, this stage representing the approximate larva–juvenile transition. Conversely, adults (666–748 dpf) show the largest disparity; the mean Procrustes distance is more than twice that of the 30-dpf stage. The same features along the series are evident visually, by comparing the consensus Procrustes shape deformations themselves (Fig. 2, the black double-headed arrows indicate the stage-matched comparisons).

A key feature of the evolutionary change in development shows up in the same diagrams by simply visually offsetting the stage matching of the oceanic and freshwater configurations by one stage, such that the 10-dpf stage for the oceanic fish (RS) is compared with the 14-dpf stage for the freshwater fish (BL), and so on through the series (Fig. 2, gray double-headed arrows). The differences between oceanic and lake

Table 1. Procrustes distances between consensus landmark configurations during development, and examining the hypothesis of pedomorphosis

	Procrustes distances*				
Stage	10 dpf	14 dpf	30 dpf	Juvenile	Adult
Comparison					
Stage-matched†	0.086	0.080	0.056	0.073	0.146
Offset-pedomorphosis‡		0.063	0.138	0.069	0.088
Offset-control§		0.129	0.194	0.109	0.102

*Data show Procrustes distances between consensus configurations for the comparisons indicated. All of the disparities differ significantly from zero ($P < 0.0001$, permutation tests implemented in MorphoJ).

†For the Stage-matched comparison, BL at the stage indicated is compared to RS at the same stage (e.g., BL at 14 dpf is compared to RS at 14 dpf).

‡For the Offset-pedomorphosis comparison, BL at the stage indicated is compared to RS at the previous stage (e.g., BL at 14 dpf is compared to RS at 10 dpf). Note that the Procrustes distance for this comparison is the lowest of all three at each stage (supporting pedomorphosis), except at the 30-dpf stage, where it is larger than the stage-matched comparison.

§For the Offset-control comparison, BL at the stage indicated is compared to BL at the previous stage (e.g., BL at 14 dpf is compared to BL at 10 dpf).

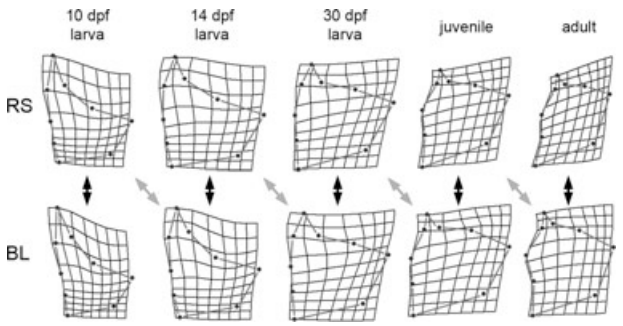

Fig. 2. Opercle shapes differ between oceanic (Rabbit Slough, RS) and freshwater (Boot Lake, BL) sticklebacks all along the entire developmental trajectories. Consensus Procrustes configurations, shown as thin plate spline deformations (scale × 1) from the overall mean configuration (across all stages) of laboratory-raised fish to the developmental stages indicated at the top. RS and BL larval stages were matched by age (days post-fertilization, dpf). The juvenile and adult stages were matched by standard lengths (fish body lengths), approximating opercle centroid sizes (see supporting information Fig. S1): RS juveniles were collected at 101 dpf, BL juveniles at 96 dpf, RS adults at 748 dpf, and BL adults at 666 dpf. The black double-headed arrows indicate sample stage-matched comparisons between the RS and BL configurations (as can be made all along the series), the gray double-headed arrows indicate offset comparisons, the offset in the direction according to a hypothesis of pedomorphosis (see text). Procrustes distances for the comparisons are given in Table 1; the four offset comparisons are generally more similar than the stage-matched ones.

now appear less prominent than for the stage-matched comparisons. This observation suggests that development in the derived form (BL) has been delayed as compared with the ancestral form (RS)—or in other words, BL development is pedomorphic. Comparing the corresponding Procrustes distances (Table 1, second row, "pedomorphosis") with the stage-matched distances (first row) supports this hypothesis of pedomorphosis: in three of the four stages, we could examine this way the offset Procrustes distance is the lower of the two values. The exception is the 30-dpf stage. If the offset pedomorphic values are compared to a control for offsetting (Table 1, second row compared with the third row), the Procrustes distances for the offset-pedomorphosis comparisons are lower for all four stages.

Multivariate regression (Fig. 3A) shows how these developmental changes in opercle shape are correlated with growth—the change in opercle size. (Regression Score in Fig. 3A refers to shape, and log CS refers to size.) Developmental allometry—covariation of shape with size—is prominent throughout the series of stages. This allometry occurs for both forms (RS, BL) with a single exception: At the very last time point, apparently no change in BL opercle shape accompanies a prominent change in BL opercle size. We note that this particular change in developmental allometry resembles the change in evolutionary allometry we examined in Fig. 1 (see Discussion). We also observe that at early stages another less-prominent difference also may be present—the rate of rise in regression score is lower for the RS fish. Using developmental time rather than size for the independent variable in the regression does not change our findings: a loss of shape change still is observed between the BL juvenile and adult stages (Fig. 3B). In contrast, shape continues to change during the same period in the oceanic fish in the oceanic, ancestral fish (RS), as the opercle grows in size. Both RS and BL fish grow in body length at about the same rate during the whole trajectory, and in both the opercle grows in size at about the same rate as well (supporting information Fig. S1). The pedomorphic change is in shape alone, and is clearly most prominent at the end of the trajectory, not constant along the entire trajectory

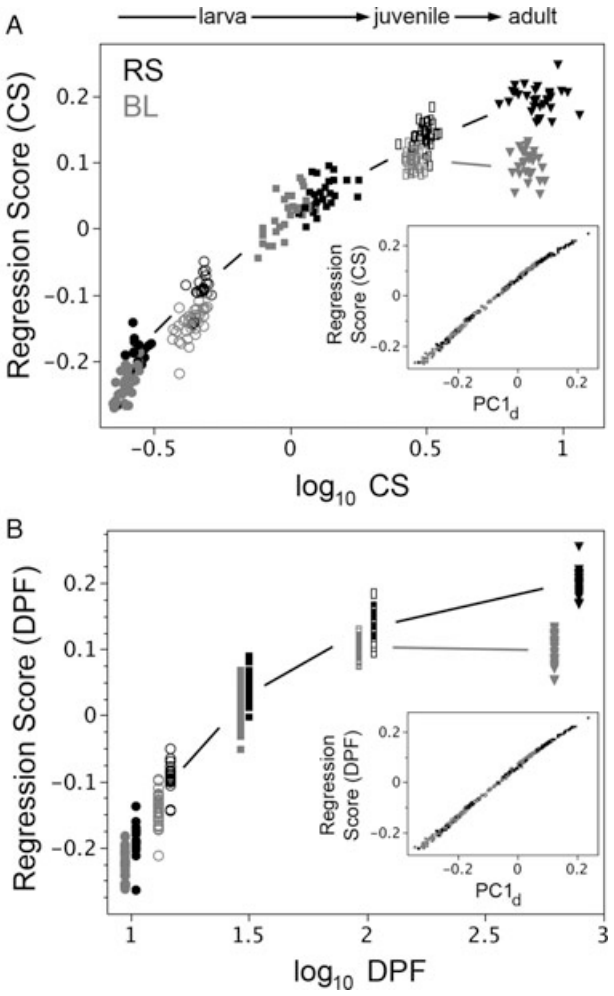

Fig. 3. The most prominent opercle shape divergence between RS (black symbols) and BL (gray) occurs late in development, as revealed by multivariate regression of shape (Regression Score) on either opercle centroid size, CS (A) or DPF (B). This divergence occurs as juvenile fish (rectangles) grow to the adult stage (triangles). In agreement, the Procrustes distances at the adult stage show the largest difference between BL and RS (Table 1, stage-matched comparisons). A less-prominent difference, showing up particularly in the allometric plot (A), is that during larval stages (10 dpf: filled circles, 14 dpf: open circles, 30 dpf: squares), the rise in Regression Score is apparently greater in BL than RS. The insets in both A and B show the high correlation between these regression vectors (Regression Scores) and $PC1_d$, the leading multivariate vector of total opercle shape variation in the RS (oceanic or ancestral) developmental dataset.

Vectors of developmental and evolutionary change line up

We computed a new set of PCs from the RS developmental series alone, yielding $PC1_d$, $PC2_d$, and so on through $PC10_d$ (the "d" denoting development), and allowing us to test a strong prediction of the hypothesis of pedomorphosis. Namely, pedomorphosis predicts that $PC1_d$, the major axis of change along the ancestral developmental trajectory, will line up with $PC1_a$, the major axis of evolutionary divergence. Importantly, we did not include the series of BL developing fish in the computation for PCA_d, for including BL would have confounded evolution and development. Because we Procrustes aligned all of the fish together (including the RS and BL developmental sets and all the adults from the various populations), we could meaningfully assign (project) PC scores from either PCA (PCA_a or PCA_d) to any of the fish, irrespective of their origins.

$PC1_d$ accounts for 75% of the total variation among opercle shapes in developing RS fish, and corresponds essentially exactly to the regression scores of opercle shape on either size or developmental time (insets in Fig. 3A and B, R^2 = 0.994 and 0.997, respectively). We also computed the vector correlations (the cosigns of the vector angles) for these relationships, and they are extremely high, 0.974 and 0.985, respectively. Hence, $PC1_d$ clearly is the major axis of ancestral developmental change, and is the precise axis needed to test our prediction. We find that, as predicted, the two vectors $PC1_d$ and $PC1_a$ are strongly correlated (vector correlation = 0.85). Bivariate plots also reveal the covariation, using either the adult dataset (Fig. 4A; $R^2 = 0.94$), or the developmental one (data not shown). Supporting information Table S1 compares the loadings of the PCs. These findings provide striking support for the hypothesis of pedomorphosis.

Figure 4B shows a result that we had not anticipated: we also see strong correlation between $PC2_d$ (explaining 11% of the opercle shape variation in the RS dataset) and $PC2_a$ (R^2 = 0.0.85, vector correlation = 0.82). As we described recently, the $PC2_a$ axis is associated with divergences among particular freshwater populations, possibly due to adaptation of the fish to local ecological regimes (Kimmel et al. 2012; see also Arif et al. 2009). The $PC2_d$:$PC2_a$ correlation indicates that evolution along PC2, like PC1, occurs by modification of an ancestral developmental axis. This modification might also be heterochronic, as we examine below. We did not find clear association between other PCs in the two datasets, as illustrated for PC3 in Fig. 4C ($R^2 = 0.06$).

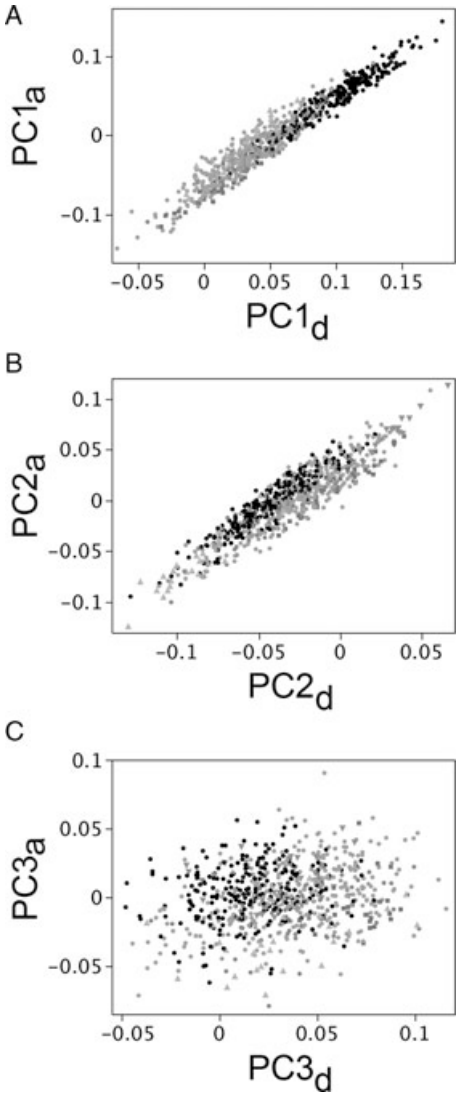

Fig. 4. The leadings axes of opercle shape variation associated with evolutionary divergence and ancestral development line up. $PC1_a$ versus $PC1_d$ (A), and $PC2_a$ versus $PC2_d$ (B) both show high correlation. In contrast, there is little or no correlation between $PC3_a$ and $PC3_d$ (C). The plots use the adult wild-captured dataset (the set shown in Fig. 1). Black points: oceanic populations. Gray points: freshwater populations.

Heterochrony is regionally dissociated

Our findings just described provide support for a heterochronic basis of opercle shape evolution. We used $PC1_d$ and $PC2_d$ in a bivariate analysis to learn whether we have a case of "classical" heterochrony (also termed "pure" heterochrony by Mitteroecker et al. 2004b) in which the developmental trajectory of shape (here opercle shape) evolves as a single entity. By single entity we mean that the entire shape of the bone is uniformly developing in a different temporal pattern in ancestor and descendant: shape is dissociated from ontogenetic stage (time), and perhaps from size (Alberch et al. 1979). Nevertheless, in this model the trajectory of opercle shape development in the derived form (BL) falls precisely along the equivalent trajectory of the ancestral form (RS) when plotted in a PC2 by PC1 shape space (Godfrey and Sutherland 1995; Mitteroecker et al. 2004a, b, 2005). We expect this correspondence because neither time nor size is included as axis in the PC2 by PC1 shape space.

A $PC2_d$ by $PC1_d$ bivariate analysis reveals that whereas the RS and BL developmental trajectories both have the forms of strongly curving sweeps across the space (Fig. 5A), the trajectories are not identical. Shape development with respect to the $PC1_d$ axis appears to have evolved in a different manner from that along the $PC2_d$ axis. Along the $PC1_d$ axis, the prominent evolutionary change in BL is a truncation that occurs at juvenile stage—the red open rectangles and red filled triangles overlap along this axis. This lack of change along $PC1_d$ is the pedomorphic change encountered above in the analysis of allometry (Fig. 3). But opercle shape development along PC2 in BL clearly is not similarly truncated at juvenile stage. The BL $PC2_d$ scores drop approximately to the same extent as the RS $PC2_d$ scores during

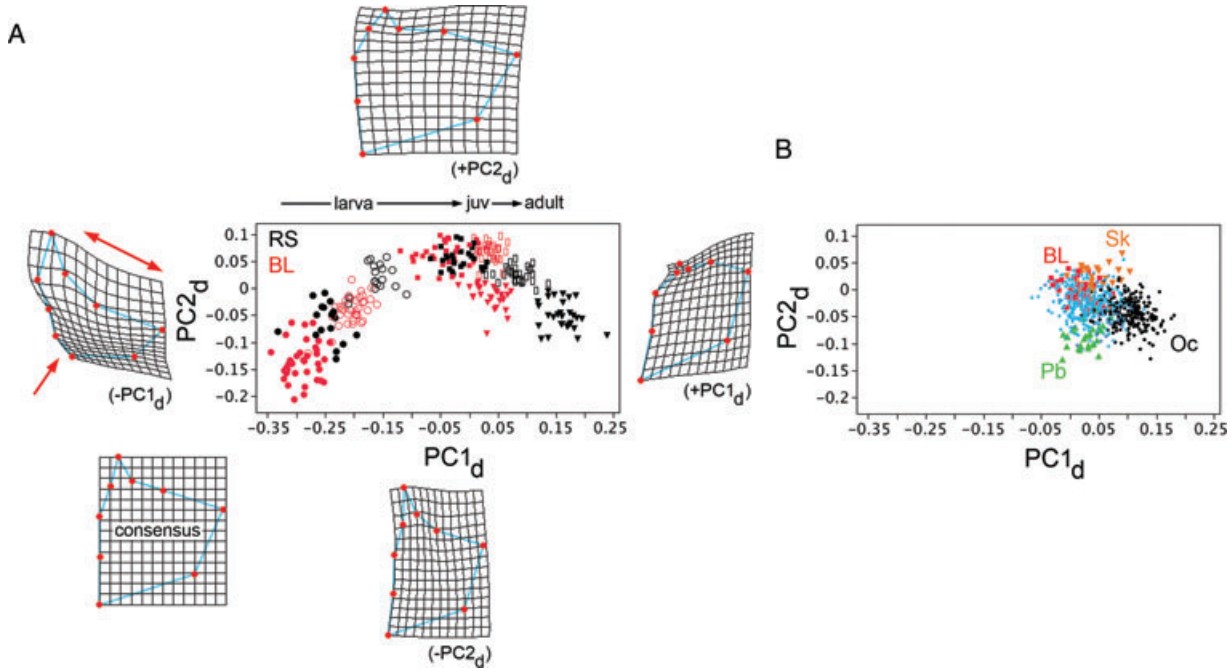

Fig. 5. Plotting opercle shape developmental trajectories (A) and adult evolutionary trajectories (B) on the same space reveals the correlations between the two. (A) Opercle development in both RS (black symbols) and BL (red) follow similar but nonmatching curving trajectories through shape space, delineated by $PC1_d$ (horizontal axis) and $PC2_d$ (vertical). Different symbols represent five different developmental stages, as in the presentation in Fig. 3. The thin plate spline diagrams surrounding the plot show the consensus configuration (RS, computed from all of the developmental stages considered together), and deformations associated with extreme high and low values of both PCs. At low $PC1_d$, characterizing the earliest developmental stages, the deformation shows dilation-diminution (red single- and double-headed arrows), that is, it is of the same nature as the evolutionary shape change characterizing divergence from the oceanic to freshwater habitats (compare with Fig. 1, supporting information Fig. S2, and see Kimmel et al., 2012). (B) For comparison with A, the adult wild-captured dataset plotted on the $PC1_d$–$PC2_d$ space, with axes and scales matching (A). Symbols match Fig. 1. BL, Boot Lake (red); Pb, Paxton Lake (green), benthic morph; Oc, oceanic (including RS and six other oceanic populations, black); Sk, Skorraddalsvatn Lake (orange). Other freshwater populations are in light blue.

this late period of development. In consequence, the adult BL opercles, in the absence of the late change along $PC1_d$, occupy a completely distinctive position in the shape space (red triangles in Fig. 5A). These data reveal regional dissociation (sensu Mitteroecker et al. 2004b) rather than classical heterochrony.

BL fish also have evolved along PC2. BL PC2 scores at the adult stage are higher than those of the RS fish, considering either the wild-captured adult (Fig. 5B, supporting information Fig. S2) or lab-reared adult datasets (Fig. 5A, triangles; $F_{1,58} = 34.1$; $P < 0.0001$). Although the late drops in $PC2_d$ scores are similar in RS and BL, the pattern is distinctive earlier, during larval development (Fig. 5A). $PC2_d$ scores are lower in BL than RS at the first (10-dpf) stage, but they rise more rapidly during larval development, to become slightly higher by the 30-dpf stage. This more rapid change in larval opercle shape development along PC2 also shows up on an allometric plot (supporting information Fig. S3). These results suggest that independent evolutionary changes in opercle shape occur along the PC1 and PC2 axes, that the shape changes are dissociated from one another, and as well dissociated from opercle CS, which has evolved only slightly, if at all (supporting information Fig. S1).

With the trajectories in Fig. 5A in mind, it is interesting to examine the evolutionary divergences among our adult wild-captured populations of fish. Figure 5B shows these divergences using the same axes and at the same scale as in A. (supporting information Fig. S2 also shows this dataset, but plotted on the $PC1_a$ and $PC2_a$ axes, and at larger scale). The cluster of black data points representing the eight oceanic populations in Fig. 5B is similar to the cluster representing RS in A, whereas the points representing freshwater populations appear to be more spread out. Notably, Icelandic Skorraddalsvatn Lake fish, with a wider opercle scoring at high PC2, and Canadian Paxton Lake benthic fish (narrower bone, low PC2) would appear to have more greatly modified aspects of PC2 development than BL fish (see Discussion).

Dissociation of the dorsal and ventral regions

How do the shape changes captured by PC1 and PC2 differ from one another? Deformation in the ventral region loads heavily on PC1 (single-headed arrow, left diagram of Fig. 5A), and the broadening of the bone at high PC2 includes the dorsal region (top diagram). Hence, we propose that a part of the dissociation revealed by our PCA is between dorsal and ventral regions of the bone. We subdivided the configuration of nine landmarks into two subsets, dorsal and ventral, to test this proposition directly, and without involving PCs (Fig. 6A): We compared Procrustes distances as measures of shape disparities of these dorsal and ventral regions specifically, between BL and RS along the developmental trajectories, just as we had done for the entire bone in Table 1. Figure 6B shows the result: the curve for the ventral region disparities matches that for the entire bone along the trajectory, disparities are lowest at the 30-dpf larval stage and rising in juveniles and adults. However, the curve for the dorsal region disparities is completely distinctive; disparities are highest in larvae, and then fall in juveniles. This result strongly supports our proposal for dorsal–ventral regional dissociation, during evolution, of opercle development.

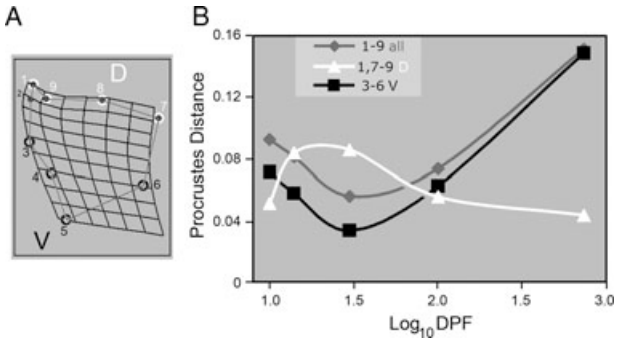

Fig. 6. Dorsal–ventral regional dissociation of opercle development between BL and RS fish. (A) We "virtually dissected" the opercle by subdividing the total landmark configuration (nine landmarks) into two landmark subsets of four landmarks each, one subset representing the dorsal (D, upper) region of the bone (landmarks 1 and 7–9), and the other subset representing the ventral (V, lower) region (landmarks 3–6). (B) The plot shows, as a function of developmental age, Procrustes distances between consensus RS and BL configurations at each stage for the three comparisons shown in the inset. We constructed the trajectories from composites of these Procrustes distances. The trajectory for the dorsal subset of landmarks (white) is distinctive from the trajectory for the ventral subset (black), supporting regional dissociation. The ventral subset is similar to the nine-landmark set for the entire bone (gray), revealing that evolution of the ventral region accounts for most of the phenotypic variation.

Dorsal–ventral dissociation may be along a module boundary

Dissociations have been used to detect, or test, the boundaries of modules, developmental or otherwise, that are generally assumed to underlie patterning of complex morphologies (e.g., Raff and Raff 2000; West-Eberhard 2003). Modules are defined by integration structure (i.e., covariances, see Wagner 1996; Hallgrímsson et al. 2009) and we examined covariances within the opercle to directly test (Klingenberg 2009; see Methods) an a priori hypothesis that its dorsal and ventral regions are separated by a module boundary. We used a new opercle landmark configuration of eight landmarks, and examined opercles at the juvenile stage, with BL and RS combined ($n = 60$). At this stage, the disparities between dorsal and ventral opercle regions are low (Fig. 6). Following the Klingenberg modularity method, we partitioned the configuration into dorsal and ventral blocks, of four landmarks each, as shown in Fig. 7. Partial least squares analysis yielded an RV coefficient, describing the strength of the covariance between these two blocks, of 0.22. This value was the very lowest for the 12 possible partitions (of four landmarks each) considered contiguous partitions using the adjacency profile shown in Fig. 7 (the highest RV was 0.46). The RV coefficient of 0.22 was the second lowest of 35 partitions in which both contiguous and noncontiguous sets of four landmarks were permitted. Alternatively, using Delaunay triangulation for the adjacency profile (the default adjacency provided by MorphoJ) did not substantially alter our findings: In this case, the RV coefficient of 0.22 was the second lowest of both 19 possible contiguous partitions and 35 contiguous and noncontiguous partitions. These tests provide direct support that the opercle is composed of dorsal and ventral modules, because by definition modules are characterized by high internal covariance structure, but are connected to other modules only weakly (Hallgrímsson et al. 2009). Hence, a partition that is not along a module boundary will yield a high RV coefficient, whereas a partition that follows a module boundary will yield a low RV coefficient, as we observe for the dorsal–ventral partition.

DISCUSSION

Sticklebacks that have independently diverged from oceanic to freshwater morphologies in geographical regions as far apart as Iceland and the eastern coast of the Pacific Ocean show a common major multivariate axis of evolution of opercle shape, PC1 (Kimmel et al. 2012). Here, we show that this axis almost exactly mirrors the major axis of ancestral opercle shape development. Mirroring is an apt term for the comparison, for the evolutionary change is opposite to the developmental one, that is, a pedomorphic shortening

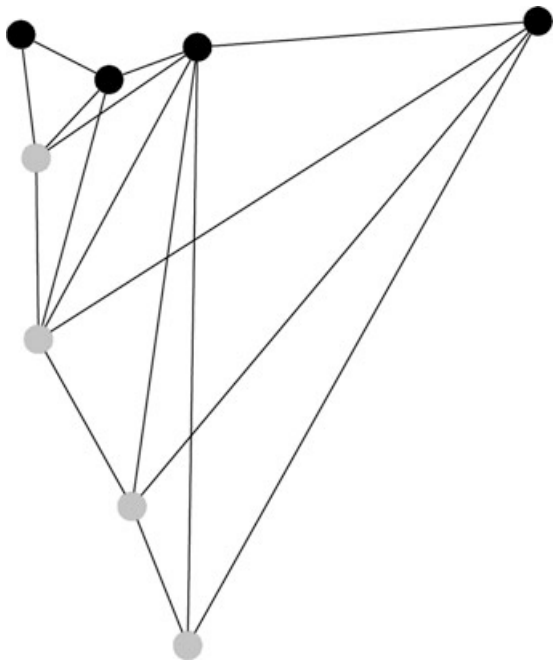

Fig. 7. Covariance structure suggests that the dorsal and ventral regions of the opercle are separated by a module boundary. Four dorsal (black) and four ventral-anterior (gray) landmarks show the two hypothetical modules. The connections between the landmarks show the adjacency profile used to determine which landmark partitions make contiguous blocks (i.e., with all landmarks in the block connected by at least one line; see Klingenberg 2009). Compared to other possible subdivisions of the configuration, and based on partial least squares analysis, the dorsal–ventral subdivision yields a very low covariance between blocks, as expected for two separate modules (see text).

of the developmental trajectory (Klingenberg 1998, see p. 84). Pedomorphosis is associated with evolutionary allometry. Shape along the PC1 axis is dissociated from bone size. Shape developments along PC1 and PC2, and in the dorsal and ventral regions of the opercle are also dissociated from one another. At least the latter might be along an opercle module boundary, as suggested from the bone's covariance structure. Dissociations and modularity may have influenced the nature of opercle evolution in stickleback, including diversification in different freshwater environments.

Pedomorphosis, dissociation, and modularity

Pedomorphosis, as usually defined (Gould 1977; Klingenberg 1998), can mean either a heterochronic shortening of a trajectory of shape development, or a slower rate of shape development along the trajectory. We clarify that in our view, the terms heterochrony and pedomorphosis refer to patterns of developmental change, not the underlying processes or mechanisms that cause timing differences (Raff and Wray 1989). Shape and size might be retarded jointly (so-called "ontogenetic scaling," Shea 1981, and see Mitteroecker et al. 2004a), or evolution might dissociate shape and size. Our evidence supports shape–size dissociation, as shape differs along the developmental trajectories between RS and BL, whereas the trajectories of opercle growth in size are almost exactly the same in the two forms (supporting information Fig. S1). The most prominent evolutionary change is that opercle shape development along PC1 stops altogether in juvenile BL fish whereas growth in bone size continues as the juveniles continue to grow to full-sized adults. Inspection of the allometric regressions (Fig. 3A, supporting information Fig. S3) also reveals other, more subtle dissociations between shape and size: At larval stages, shape developments along both PC1 and PC2 are evidently more rapid relative to size in BL than in RS—the opposite of a pedomorphic change.

Portraying the trajectories on a PC2 by PC1 space (Fig. 5A, a "shape space" as neither size nor time is plotted) reveals a different kind of dissociation—one between shape along PC1 and shape along PC2. With uniform heterochronic change in shape development, the RS and BL fish would fall along the same trajectory in a PC1 by PC2 shape space (Godfrey and Sutherland 1995; Mitteroecker et al. 2004a, b, 2005). But the nonmatching trajectories we observe in this space suggest regionally dissociated heterochrony, in the sense proposed by Mitteroecker et al. 2004b. Only a one of the shape differences, the prominent PC1 change at juvenile stage, shows a clear pedomorphic signal.

It is likely that part of dissociation revealed by PCA corresponds to the dorsal–ventral dissociation revealed by "virtual" dissection (Fig. 6). Dissociation appears to occur along a module boundary, as evidenced by examination of the opercle's covariance structure by partial least squares analysis. It is interesting to consider how the opercle evolves in shape between oceanic and freshwater fish in this light. The pedomorphic pattern captured by PC1 is that the derived adult form in freshwater sticklebacks is expanded along the dorsal edge, a change that we have termed "dilation" above and in previous publications (Kimmel et al. 2008, 2012), and is compressed ventrally (diminution). These two prominent changes, if the above interpretations are valid, occur in separate modules. The fact that dilation-diminution is captured by the leading eigenvector characterizing the phenotypic change between oceanic and freshwater fish (namely $PC1_a$) means, of course, that the two changes have strongly covaried during evolution. Yet separate modules, by definition, are joined by only weak covariance structure. Although this contrast would seem to present us with a dilemma, in fact it does not. The inference seems clear: a major role of the covariance structure, including modularity, in constraining the direction of evolutionary change is not supported. Recently, we carried out a quantitative genetic experiment to address whether ancestral genetic architecture may have biased the direction of evolution. We found little support for this hypothesis, and proposed that

directional selection was the more likely explanation for parallel evolution to the freshwater phenotype (Kimmel et al. 2012). The current study goes further in suggesting the hypothesis that correlational selection, rather than strong associations during development, results in the observed covariation between dorsal and ventral components of opercle shape across populations.

Developmental and evolutionary allometry—two sides of the same coin

Allometry, not to be confounded with heterochrony (Klingenberg 1998) but arguably connected to it (Gould 1977), refers to the relationship between size and shape. We show that allometry has evolved between oceanic and freshwater stickleback, a subject of some interest currently (Klingenberg 2010). Two kinds of allometry are of interest in this study—evolutionary allometry, where one compares the size–shape relationships among related populations, and developmental (ontogenetic) allometry, for which one examines a developmental trajectory (review; Klingenberg 1998). We compared the two, and our data suggest they coincide. The developmental change from allometric growth to nearly isometric growth by juvenile BL fish (Fig. 3A, supporting information Fig. S3) is apparently matched by evolutionary allometry across populations (Fig. 1). $PC1_a$, capturing evolutionary allometry, and $PC1_d$, capturing developmental allometry and computed from an entirely different dataset, are equivalent (Fig. 4A). The inference is clear: the cessation of shape development along PC1 at juvenile stage not only occurs in the lab-reared BL population we examined, but occurs in native freshwater populations on a global scale. By this interpretation, parallel evolution of opercle shape in independent populations shows the same developmental pattern of change. Our proposal that a pedomorphic truncation of development at juvenile stage accounts for parallel evolution of opercle shape in stickleback could readily be tested further by examining development of oceanic–freshwater pairs of fish (as we have done here for the two Alaskan populations) collected from locations geographically distant from Alaska.

Dissociation may underlie shape divergences among freshwater populations

Besides the PC1 differences, the BL fish we examine in our laboratory common-garden developmental analysis also show developmental differences from oceanic RS fish along the PC2 axis. Most notably, the early rise in PC2 is larger in BL (best shown in supporting information Fig. S3B). This rise and subsequent fall in both morphs exemplify what Hallgrímsson et al. (2009) refer to as the "palimpsest." In this palimpsest model, developmental changes occurring early in a trajectory are obscured—overwritten by changes occurring later. In our case, as captured by PC2, anterior–posterior widening of the opercle during the early part of the trajectory is then erased by its narrowing again after the larva–juvenile transition (Fig. 5A,supporting information Fig. S3B). One can identify the same widening, then narrowing of the bone in the diagrams in Fig. 2, which show of complete Procrustes deformations, and serve to reveal that the palimpsest-like change is not an artifact of just looking along the single PC2 axis. We think this is not a trivial example because the pattern appears to be conserved evolutionarily: We see the same sort of rise and fall along a PC2 axis in a study of shape development of the opercle in zebrafish (Kimmel et al. 2010). Stickleback (a percomorph), and zebrafish (an ostariophysan) are not at all closely related among the 30,000 or so species of teleosts, their lineages are thought to have diverged about 180 Ma (Santini et al. 2009). Yet in both species, the PC2 peak is near the larva–juvenile transition and represents broadening of the bone, then subsequently narrowed. Further study will be required to learn the significance of the developmental rise and fall along PC2. Such study could be of some interest because particular lake populations, which we have examined only as adults, have diverged along the PC2 axis (Fig. 5B, supporting information Fig. S2). We can speculate that the developmental trajectory of Icelandic Skorraddalsvatn Lake fish, with a wide bone scoring high on PC2, might further amplify the same rapid PC2 rise we observe in BL larvae. Alternatively, this population might omit (truncate) the sharp PC2 drop we observe for BL and RS juveniles. The trajectory of Canadian Paxton Lake benthic fish scoring low on PC2 might have exaggerated the PC2 drop (thus yielding a narrow bone). Whether these speculations have merit can be examined directly by carrying out developmental studies with fish obtained from these freshwater populations.

Prospects

A challenge for the field of evo devo is to understand the molecular-genetic and cellular underpinnings of how dissociations and modularity are achieved. A promising approach is in-depth studies in natural populations of traits, such as the opercle, for which the genetic and cellular underpinnings are at least partially known, from work on model organisms in the laboratory. This is the case for the opercle, where, as pointed out in the Introduction, we have detailed information from zebrafish about opercle cellular morphogenesis, and molecular evidence for modularity. In fact, the zebrafish hedgehog study (Huycke et al. 2012) provides a candidate molecular pathway for the dorsal–ventral modularity we support in this study; Ihha regulates development of a ventral module. Identifying whether modularity at the level of gene regulation and cellular behavior translates into phenotypic patterns of integration and

dissociation (sensuWagner 1996; Wagner and Altenberg 1996; Mezey et al. 2000) will be an area of intense research in coming years in both model and nonmodel organisms. With genomic tools quickly becoming available for stickleback (Kingsley et al. 2004; Cresko et al. 2007; Miller et al. 2007; Hohenlohe et al. 2010), the time would seem ripe for extending this kind of understanding to problems of dissociation and modularity underlying natural variation in skeletal development.

Acknowledgments

We thank Brian Eames, Benedikt Hallgrímsson, and Katrina McGuigan for detailed comments on the manuscript, and to Heather Jamniczky for providing helpful suggestions concerning methods of data analysis. The research was funded by US National Science Foundation grants IOS-0818738 and IOS-0642264. PAH also received support from NIH/NCRR grant P20RR16448 (L. Forney, P.I.).

REFERENCES

Alberch, P., Gould, S. J., Oster, G. F., and Wake, D. B. 1979. Size and shape in ontogeny and phylogeny. *Paleobiology* 5: 296–317.

Arif, S., Aguirre, W. E., and Bell, M. A. 2009. Evolutionary diversification of opercle shape in Cook Inlet threespine stickleback. *Biol. J. Linn. Soc.* 97: 832–844.

Atchley, W. R., and Hall, B. K. 1991. A model for development and evolution of complex, morphological structures. *Biol. Rev.* 66: 101–157.

Bell, M. A., and S. A. Foster. (eds.) 1994. *The Evolutionary Biology of the Threespine Stickleback*. Oxford University Press, Oxford.

Cheverud, J. M. 1996. Developmental integration and the evolution of pleiotropy. *Am. Zool.* 36: 44–50.

Cresko, W., McGuigan, K. and Phillips, P. 2007. Studies of threespine stickleback developmental evolution: progress and promise. *Genetica* 129: 105–126

Godfrey, L. R., and Sutherland, M. R. 1995. What's growth got to do with it? Process and product in the evolution of ontogeny. *J. Hum. Evol.* 29: 405–431.

Gould, S. J. 1977. *Ontogeny and Phylogeny*. Harvard University Press, Cambridge.

Gregory W. K. 1933. *Fish Skulls: A Study of the Evolution of Natural Mechanisms*. The American Philosophical Society, Philadelphia, PA.

Hallgrímsson, B., et al. 2009. Deciphering the palimpsest: studying the relationship between morphological integration and phenotypic covariation. *Evol. Biol.* 36: 355–376.

Hohenlohe, P. A., Bassham S., Etter, P. D., Stiffler, N., Johnson, E. A., and Cresko, W. A. 2010. Population genomics of parallel adaptation in threespine stickleback using sequenced RAD tags. *PLoS Genetics* 6: e1000862.

Huycke, T. R., Eames, B. F., and Kimmel, C. B. 2012. Hedgehog-dependent proliferation drives modular growth during morphogenesis of a dermal bone. *Development* 139: 2371–2380.

Kimmel, C. B., Aguirre, W. E., Ullmann, B., Currey, M., and Cresko, W. A. 2008. Allometric change accompanies opercular shape evolution in Alaskan threespine sticklebacks. *Behaviour* 145: 669–691.

Kimmel, C. B., DeLaurier, A., Ullmann, B., Dowd, J., and McFadden, M. 2010. Modes of developmental outgrowth and shaping of a craniofacial bone in zebrafish. *PLoS ONE* 5: e9475.

Kimmel, C. B., et al. 2012. Independent axes of genetic variation and parallel evolutionary divergence of opercle bone shape in threespine stickleback. *Evolution* 66: 419–434.

Kimmel, C. B., et al. 2005. Evolution and development of facial bone morphology in threespine sticklebacks. *Proc. Natl. Acad. Sci. USA* 102: 5791–5796.

Kimmel, C. B., Ullmann, B., Walker, M., Miller, C. T., and Crump, J. G. 2003. Endothelin 1-mediated regulation of pharyngeal bone development in zebrafish. *Development* 130: 1339–1351.

Kingsley, D., et al. 2004. New genomic tools for molecular studies of evolutionary change in threespine sticklebacks. *Behaviour* 141: 1331–1344.

Klingenberg, C. P. 1998. Heterochrony and allometry: the analysis of evolutionary change in ontogeny. *Biol. Rev.* 73: 79–123.

Klingenberg, C. P. 2009. Morphometric integration and modularity in configurations of landmarks: tools for evaluating a priori hypotheses. *Evol. Dev.* 11: 405–421.

Klingenberg, C. P. 2010. There's something afoot in the evolution of ontogenies. *BMC Evol. Biol.* 10: 221.

Klingenberg, C. P. 2011. MorphoJ: an integrated software package for geometric morphometrics. *Mol. Ecol. Res.* 11: 353–357.

Makinen, H. S., Cano, J. M., and Merila, J. 2006. Genetic relationships among marine and freshwater populations of the European three-spined stickleback (*Gasterosteus aculeatus*) revealed by microsatellites. *Mol. Ecol.* 15: 1519–1534.

Mezey, J., Cheverud, J., and Wagner, G. 2000. Is the genotype-phenotype map modular? A statistical approach using mouse quantitative trait loci data. *Genetics* 156: 305–311.

Miller, C. T., Beleza, S., Pollen, A. A., Schluter, D., Kittles, R. A., Shriver, M. D., and Kingsley, D. M. 2007. cis-Regulatory changes in Kit ligand expression and parallel evolution of pigmentation in sticklebacks and humans. *Cell* 131: 1179–1189.

Miller, C. T., Swartz, M. E., Khuu, P. A., Walker, M. B., Eberhart, J. K., and Kimmel, C. B. 2007b. mef2ca is required in cranial neural crest to effect Endothelin1 signaling in zebrafish. *Dev. Biol.* 208: 144–157.

Mitteroecker, P., Gunz, P., Bernhard, M., Schaefer, K., and Bookstein, F. L. 2004a. Comparison of cranial ontogenetic trajectories among great apes and humans. *J. Hum. Evol.* 46: 679–698.

Mitteroecker, P., Gunz, P., and Bookstein, F. L. 2005. Heterochrony and geometric morphometrics: a comparison of cranial growth in *Pan paniscus* versus *Pan troglodytes*. *Evol. Dev.* 7: 244–258.

Mitteroecker, P., Gunz, P., Weber, G. W., and Bookstein, F. L. 2004b. Regional dissociated heterochrony in multivariate analysis. *Ann. Anat.* 186: 463–470.

Needham, J. 1933. On the dissociability of the fundamental process in ontogenesis. *Biol. Rev.* 8: 180–223.

Raeymaekers, J. A., Maes, G. E., Audenaert, E., and Volckaert, F. A. 2005. Detecting Holocene divergence in the anadromous-freshwater three-spined stickleback (*Gasterosteus aculeatus*) system. *Mol. Ecol.* 14: 1001–1014.

Raeymaekers, J. A., Van Houdt J. K., Larmuseau, M. H., Geldof, S., and Volckaert, F. A. 2007. Divergent selection as revealed by Pst and QTL-based Fst in three- spined stickleback (*Gasterosteus aculeatus*) populations along a coastal-inland gradient. *Mol. Ecol.* 16: 891–905.

Raff, E. C., and Raff, R.A. 2000. Dissociability, modularity, evolvability. *Evol. Dev.* 2: 235–237.

Raff, R. A. 1996. *The Shape of Life. Genes, Development, and the Evolution of Animal Form*. University of Chicago Press, Chicago, p. 520.

Raff, R. A., and Wray, G. A. 1989. Heterochrony: Developmental mechanisms and evolutionary results. *J. Evol. Biol.* 2: 409–434.

Rohlf, F. 2004. *Thin-Plate Spline*, version 1.20 (computer software). Department of Ecology and Evolution, State Univ. of New York at Stony Brook.

Rohlf, F. 2008a. *tpsDig2, Digitize Landmarks and Outlines*, version 2.12 (computer software). Department of Ecology and Evolution, State Univ. of New York at Stony Brook.

Rohlf, F. 2008b. *tpsRelw, Relative Warps Analysis*, version 1.46 (computer software). Department of Ecology and Evolution, State Univ. of New York at Stony Brook.

Santini, F., Harmon, L. J., Carnevale, G., and Alfaro, M. E. 2009. Did genome duplication drive the origin of teleosts? A comparative study of diversification in ray-finned fishes. *BMC Evol. Biol.* 9:194. doi:10.1186/1471-2148-9-194.

Shea, B. T. 1981. Relative growth of the limbs and trunk in the African apes. *Am. J. Phys. Anthropol.* 56: 179–201.
Talbot, J. C., Johnson, S. L., and Kimmel, C. B. 2010. *hand2* and Dlx genes specify dorsal, intermediate and ventral domains within zebrafish pharyngeal arches. *Development* 137: 2507–2517.
Wagner, G. P. 1996. Homologues, natural kinds and the evolution of modularity. *Am. Zool.* 36: 36–43.
Wagner, G., and Altenberg, L. 1996. Complex adaptations and the evolution of evolvability. *Evolution* 50: 967–976.
Warton, D. I., Wright, I. J., Falster, D. S., and Westoby, M. 2006. Bivariate line-fitting methods for allometry. *Biol. Rev.* 81: 259–291.
West-Eberhard, M. J. 2003. *Developmental Plasticity and Evolution*. Oxford University Press, Oxford.
Zelditch, M. L., Swiderski, D. L., Sheets, H. D., and Fink, W. L. 2004. *Geometric Morphometrics for Biologists: A Primer*. Elsevier Academic Press, London.
Zelditch, M. L., Wood, A. R., Bonett, R. M., and Swiderski, D. L. 2008. Modularity of the rodent mandible: Integrating bones, muscles, and teeth. *Evol. Dev.* 10: 756–768.

SUPPORTING INFORMATION

Additional Supporting Information may be found in the online version of this article:

Figure S1. Size measurements along the developmental trajectories do not differ substantially between RS (black symbols) and BL (red).

Figure S2. Evolutionary divergence among habitats (oceanic, freshwater) and freshwater populations (BL, Pb, Sk, and others) plotted on a shape space defined by the PC1a and PC2a axes.

Figure S3. Shape–size spaces of opercle development constructed by plotting PC1d scores (A, note the similarity of this plot to Fig. 3A in the main text), and PC2d scores (B) versus CS

Table S1. Loadings (eigenvalues) for the first three principal components of the developmental (d) and adult wild-captured (a) datasets.

Please note: Wiley-Blackwell are not responsible for the content or functionality of any supporting materials supplied by the authors. Any queries (other than missing material) should be directed to the corresponding author for the article.